Effect of Ag and Au Nanoparticles on the SERS of 4-Aminobenzenethiol Assembled on Powdered Copper

Kwan Kim* and Hyun Sook Lee

Laboratory of Intelligent Interfaces, School of Chemistry, Seoul National University, Seoul 151-742, Korea

Received: May 20, 2005; In Final Form: August 16, 2005

Raman scattering measurements were conducted for 4-aminobenzenethiol (4-ABT) assembled on powdered copper substrates. Initially, very weak Raman peaks were detected, but upon attaching Ag nanoparticles probably via NH_2 groups onto 4-ABT/Cu, distinct Raman spectra were observed. Considering the fact that no Raman peak was identified when Ag nanoparticles were adsorbed on 4-aminophenyl-derivatized silane monolayers assembled on silica powders, the Raman spectra observed for Ag@4-ABT/Cu should be surface-enhanced Raman scattering (SERS) spectra, occurring by an electromagnetic coupling of the localized surface plasmon of Ag nanoparticles with the surface plasmon polariton of Cu powders. The extra enhancement factor attainable by the attachment of a single Ag nanoparticle is estimated to be as large as 1.4×10^5 in the case when 632.8-nm radiation is used as the excitation source. When Au nanoparticles were attached onto 4-ABT/Cu, at least an order of magnitude weaker Raman spectra were obtained at all excitation wavelengths, however, indicating that the Au-to-Cu coupling should be far less effective than the Ag-to-Cu coupling for the induction of SERS.

1. Introduction

Noble metallic nanostructures exhibit a phenomenon known as surface-enhanced Raman scattering (SERS) in which the scattering cross-sections are dramatically enhanced for molecules adsorbed thereon.[1,2] In recent years, it has been reported that even single-molecule spectroscopy is possible by SERS,[3−5] suggesting that the enhancement factor can reach as much as $10^{14}-10^{15}$. According to theoretical studies, at least 8−10 orders of magnitude must arise from electromagnetic surface plasmon excitation,[5,6] while the enhancement factor due to the chemical effect is presumed to be of the order of 10^1-10^2.[7−9]

In agreement with the electromagnetic and chemical enhancement mechanisms, SERS is especially sensitive to the first layer of adsorbates. Accordingly, SERS has found important applications in many areas of chemistry, including chemical analysis, corrosion, lubrication, and heterogeneous catalysis.[10−14] However, SERS has not developed to be as powerful a surface technique as many people had hoped initially because of two specific obstacles.[2] One obstacle is that only noble metals such as Ag and Au can provide large enhancement, severely limiting the widespread applications involving other metallic materials of both fundamental and practical importance. The other major obstacle is that, even for those noble metals, surface morphology with a roughness scale of 50−200 nm is crucial for exhibiting a large enhancement factor.

To use SERS in routine, on-line studies for analytical purposes, SERS spectra should be obtainable even for the molecules anchored on solid surfaces with negligible SERS activity. We believe that surface Raman spectra can be obtained if Ag or Au nanoaggregates are assembled at the gaps/crevices of organic monolayers. We also think that at least when the underlying substrate is metallic, the surface Raman spectra can be acquired by attaching Ag (or Au) nanoparticles at the terminal part of the organic monolayer so as to form a nanosized gap between the underlying substrate and metal nanoparticles. Recently, Zheng et al.[15] reported that a SERS spectrum could be obtained for 4-aminobenzenethiol (4-ABT) adsorbed on a macroscopically smooth silver metal by assembling nanosized Ag particles thereon. We have examined in this work whether Ag and Au nanoparticles are also able to induce SERS for 4-ABT assembled on weakly SERS-active copper powders. Enhanced Raman spectra were indeed observed not only by Ag nanoparticles but also by Au nanoparticles. However, a Raman spectrum at least an order of magnitude weaker was obtained at all excitation wavelengths (through 488 and 647 nm) by Au nanoparticles, indicating that the Ag-to-Cu coupling should be more effective than the Au-to-Cu coupling for the induction of SERS. More importantly, the system considered in this study is mimicking a situation wherein molecules are captured inside nanosized gaps (crevices) formed between metal nanoparticles and a copper substrate underneath. In fact, we found that the Raman peak of 4-ABT on Cu could be enhanced by as much as 1.4×10^5 times by attaching a single Ag nanoparticle onto 4-ABT/Cu. These observations clearly support the current contention[5,6,15,16] that the crevices or the gaps of two or three nanoparticles in contact with one another must be "hot" sites for the induction of SERS via a huge EM enhancement mechanism.

2. Experimental Section

4-Aminobenzenethiol (4-ABT, 97%), silver nitrate (99.998%), sodium citrate (99%), tetrachloroauric acid (98%), and copper powder (μCu, 99.9+% purity) with a nominal particle size of 2−3.5 μm were purchased from Aldrich and used as received. (4-Aminophenyl)trimethoxysilane (4-APTMS, 90%) and silica powder (1.5 μm, 99.9%) were purchased from Gelest and Lancaster, respectively, and also used as received. Copper powders were washed consecutively with ethanol (Merck, 99%); this was performed only to clean the copper powders and to remove any carbon impurities thereon. Stock solutions of 20

* To whom all correspondence should be addressed. Phone: +82-2-8806651. Fax: +82-2-8891568. E-mail: kwankim@snu.ac.kr.

10.1021/jp052665z CCC: $30.25
Published on Web 09/20/2005

mM 4-ABT in ethanol were bubbled with nitrogen before use. Chemicals otherwise specified were reagent grade, and highly pure water, of resistivity greater than 18.0 MΩ·cm (Millipore Milli-Q System), was used in making aqueous solutions.

Ag sol was prepared by following the recipes of Lee and Meisel.[17] Initially, an amount of 100 mL of silver nitrate solution containing 17 mg of $Ag(NO_3)$ was brought to the boil. A solution of 1% sodium citrate (2 mL) was then added to the $AgNO_3$ solution under vigorous stirring, and boiling was continued for ~30 min. To prepare Au sol having the same size as Ag sol, a 50 mL amount of tetrachloroauric acid solution containing 5 mg of Au was brought to the boil. A solution of 1% sodium citrate (0.4 mL) was added to the $HAuCl_4$ solution under vigorous stirring, and boiling was continued for 30 min. The Ag and Au sol solutions thus prepared were stable for several weeks, and the nanoparticles obtained were all spherical with average diameters of ~50 nm.

For the self-assembly of 4-ABT on copper, 0.050 g of copper powder was placed in a small vial into which 1.5 mL of the stock solution of 4-ABT (20 mM ethanolic solution) was subsequently added. After 12 h, the solution phase was decanted. The remaining solid particles were left to dry in a vacuum for 2 h. For attaching Ag or Au nanoparticles to the pendent NH_2 groups of 4-ABT/Cu, the powdered samples were soaked in Ag or Au sols for 3 h; the volume of each of the two sols was adjusted to contain an equal number of nanoparticles. After washing with water and ethanol consecutively, the samples were left to dry in a vacuum for 2 h and then subjected to Raman spectral analyses.

For a control experiment, 4-aminophenyl-derivatized silica beads were prepared. Initially, 1.5-μm-sized silica beads were treated with "piranha solution" (a 3:1 mixture of H_2SO_4 and H_2O_2) in an ultrasonic bath for 30 min. They were then rinsed thoroughly with deionized water and dried in a vacuum for 2 h. Cleaned silica beads were rinsed further with, in order, methanol, a mixture of methanol and toluene (1:1 in volume), and pure toluene. A 1-g amount of cleaned silica beads was dispersed in 45 mL of toluene by stirring, and then 5 mL of 10% 4-APTMS in toluene was added dropwise to the suspension, stirring further in atmosphere for 24 h. The silica beads were separated from the suspension by centrifugation and washed consecutively with toluene, a 1:1 mixture of toluene/methanol, and methanol. After drying in a vacuum, the silica beads were calcined at 140 °C for 3 h under an N_2 atmosphere. To attach Ag nanoparticles to the pendent NH_2 groups, the beads were soaked in Ag sol for 3 h. After washing with water and ethanol, they were left to dry in a vacuum for 2 h and then subjected to Raman spectral analyses.

For another control experiment, we have obtained SERS spectra of 4-ABT and 4-APTMS in aqueous Ag sol. Initially, an ethanol solution of 4-ABT or 4-APTMS was added to the Ag sol to give a final adsorbate concentration of 2×10^{-5} M. When the aggregation of silver sol particles did not occur easily, a small amount of $BaCl_2$ was added to induce the aggregation. After the sol solution changed from grayish-yellow to bluish-green, poly(vinylpyrolidone) (PVP, MW 360 000) was added as a colloid stabilizer whose concentration was 0.01% in the final solution.

Raman spectra were obtained using a Renishaw Raman system Model 2000 spectrometer equipped with an integral microscope (Olympus BH2-UMA). The 488 and 514.5 nm lines from a 20 mW Ar^+ laser (Melles-Griot Model 351MA520) or the 568 and 647 nm lines from a 20 mW Ar^+/Kr^+ laser (Melles-Griot Model 35KAP431) or the 632.8 nm line from a 17 mW

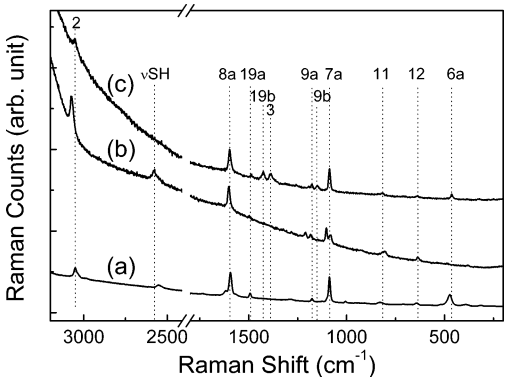

Figure 1. Normal Raman spectra of 4-ABT taken using 488-nm radiation as excitation source (a) in neat solid state, (b) in acidic (pH 4), and (c) in alkaline (pH 10) solutions.

He/Ne laser (Spectra Physics Model 127) were used as the excitation source. A glass capillary was used as a sampling device, and Raman scattering was detected with 180° geometry with a Peltier cooled (−70 °C) charge-coupled device (CCD) camera (400 × 600 pixels). The laser beam was focused onto a spot approximately 1 μm in diameter with an objective microscope with magnification of the order of 20×. The data acquisition time was usually 30 s. The holographic grating (1800 grooves/mm) and the slit allowed the spectral resolution to be 1 cm^{-1}. The Raman band of a silicon wafer at 520 cm^{-1} was used to calibrate the spectrometer, and the accuracy of the spectral measurement was estimated to be better than 1 cm^{-1}.

Field emission scanning electron microscope (FE-SEM) images of copper powders were obtained with a JSM-6700F FE-SEM operated at 5.0 kV. UV/vis spectra of Ag and Au sols were obtained with a SCINCO S-2130 spectrometer. Transmission electron microscope (TEM) images of these sols were obtained with a JEM-200CX transmission electron microscope at 200 kV after placing a drop of the as-prepared sol onto Ni/Cu grids. Nitrogen adsorption/desorption isotherms of neat copper powders were measured at 77 K using a Micromeritics ASAP 2000 system, and the surface area was determined by referring to the BET (Brunauer−Emmett−Teller) equation.[18]

3. Results and Discussion

4-Aminobenzenethiol was chosen as a probing adsorbate on the grounds of our preliminary observations that the molecule was adsorbed very favorably on copper by forming a Cu−thiolate bond and Ag and Au nanoparticles could be bound subsequently to the pendent amine groups.

To help interpret the Raman spectra of 4-ABT on copper, the normal Raman (NR) spectra of 4-ABT in pure solid state and in acidic (pH 4) and alkaline (pH 10) solutions were taken. The spectral pattern of each species was barely dependent on the excitation wavelengths from 488 to 647 nm. Parts a−c of Figure 1 represent the NR spectra of those species, respectively, obtained using 488-nm radiation as the excitation source. The spectral differences in these figures can be attributed mainly to the protonation of amine in acidic solution and/or to the deprotonation of thiol in alkaline solution. The vibrational peak assignments are summarized in Table 1.

Raman spectra could be obtained for 4-ABT assembled on copper powders but with very low signal-to-noise ratios. The spectral pattern, although weak, was dependent on the excitation wavelengths. Two typical Raman spectra taken for 4-ABT/Cu using 488- and 647-nm radiation as the excitation sources are shown in Figure 2a,b. For reference, the background spectra

TABLE 1: Raman Spectral Peak Assignments of 4-Aminobenzenethiol[a]

normal Raman			SERS			
solid	acidic	basic	4-ABT/Cu	Ag@4-ABT/Cu	Au@4-ABT/Cu	assignmt[b]
3368w						ν_{as}(NH)
3205vw						ν_{s}(NH)
3050m	3076s	3055w				ν(CH), 2(a_1)
3036sh						ν(CH), 13(a_1)
2552w	2580m					ν(SH)
1618w						δ(NH)
1593s	1601s	1598s	1597sh	1589sh	1595sh	ν(CC), 8a(a_1)
1570w			1574m	1574s	1574m	ν(CC), 8b(b_2)
1493w	1497vw	1485vw	1489sh	1490w	1489m	ν(CC) + δ(CH), 19a(a_1)
			1473w	1472w	1473vw	
		1425m	1438m	1436s	1439s	ν(CC) + δ(CH), 19b(b_2)
		1387m	1392m	1390s	1393s	ν(CC) + δ(CH), 3(b_2)
			1380sh	1375sh	1373sh	
1315vw			1303vw	1309vw	1311w	ν(CC) + δ(CH), 14(b_2)
1289vw						ν(CH), 7a (a_1)
			1255vw	1232vw		
	1209w				1218vw	
			1191vw	1190w	1194w	
1177w	1184w	1177w		1171w	1172w	δ(CH), 9a(a_1)
		1151w	1151m	1141s	1140m	δ(CH), 9b(b_2)
			1141m			
1099sh	1103s					
1088s	1083m	1087s	1078m	1073s	1078m	ν(CS), 7a(a_1)
1007w			1003vw	1004vw	1008w	γ(CC) + γ(CCC), 18a(a_1)
940vw						π(CH), 17a(a_2)
					925vw	π(CH), 5b(b_1)
910vw						δ(SH)
829w			828vw			π(CH), 10a(a_2)
820sh	817sh	819vw	818vw	820vw	819vw	π(CH), 11(b_1)
	804w		809vw			γ(CH) + γ(CS) + γ(CC) (a_1)
				750vw	750vw	π(CH), 10b(b_2)
711vw				713w	710vw	π(CH) + π(CS) + π(CC), 4b(b_1)
642w	636w	636vw	635w	640w	634w	γ(CCC), 12(a_1)
520vw			525vw	535w	530vw	γ(CCC), 16b(b_1)
473m		462w				γ(CCC), 6a(a_1)
				440vw	447vw	
391vw			405vw	405w	410vw	τ(CC), 16a(a_2)
314vw						δ(CH) + δ(CS), 18b(b_2)

[a] vs, very strong; s, strong; m, medium; w, weak; and vw, very weak. [b] Assignment is made by consulting refs 19 and 20, denoting the following: ν, stretch; δ and γ, bend; π, wagging; and τ, torsion. The ring modes correspond to those of benzene under C_{2v} symmetry.

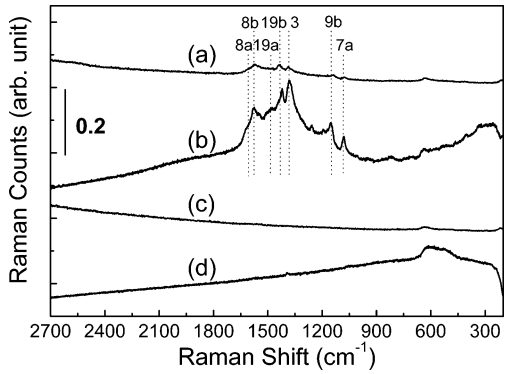

Figure 2. SERS spectra of 4-ABT on powdered copper measured at (a) 488-nm and (b) 647-nm excitation. Spectra c and d correspond to Raman spectra of neat Cu powder obtained at 488- and 647-nm excitation, respectively.

taken for neat Cu powder are also shown in Figure 2c,d. The Raman scattering intensities in these figures are referenced with respect to those for silicon wafers used for instrument calibration. The featureless as well as noisy and scattered peaks in Figure 2c,d are due to the hydrocarbon contamination of powdered copper in the ambient conditions. The peaks in Figure 2a,b are clearly due to 4-ABT adsorbed on copper, as summarized in Table 1. The S−H stretching peak is completely absent in these figures, reflecting the fact that 4-ABT is adsorbed on Cu as thiolate after deprotonation of the thiol group. The four peaks at 1574, 1438, 1392, and 1141 cm^{-1} can be assigned to ring 8b, 19b, 3, and 9b modes of 4-ABT, respectively, that possess the b_2-type of symmetry,[19,20] while the peaks at 1597, 1489, and 1078 cm^{-1} are due to 8a, 19a, and 7a modes, respectively, possessing the a_1-type of symmetry.[19,20] It is very intriguing that b_2-type bands are clearly seen in the Raman spectra of 4-ABT/Cu although their counterparts are invisibly weak in the NR spectra in Figure 1. It is also noteworthy that the relative peak intensity of the a_1-type band, for instance, at 1078 cm^{-1} is dependent on the excitation wavelengths. The overall peak intensity of 4-ABT/Cu also increases upon an increase of the excitation wavelength. All of these peculiar features are presumed to be due to the charge-transfer (CT) phenomenon between 4-ABT and copper substrate. It is well-known that Raman scattering enhancement up to an order of 10^2 can readily occur via the CT mechanism.[7−9] Since the Cu powders used in this work are not efficient substrates to show large electromagnetic enhancement, peaks due to CT enhancement are thought to appear exclusively. The enhancement factor (EF) value estimated by referring to the b_2-type band (ν_3) in Figures 2a and 1c is as large as ∼100, while the value estimated from the a_1-type band (ν_{7a}) is ∼15.

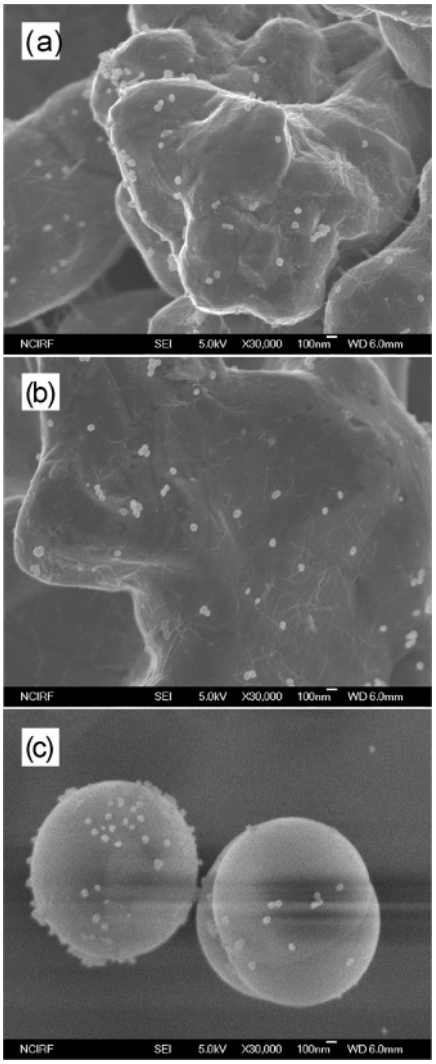

Figure 3. FE-SEM images of (a) Ag@4-ABT/Cu, (b) Au@4-ABT/Cu, and (c) Ag@4-APTMS/SiO_2.

Figure 3a shows the FE-SEM image of 4-ABT/Cu after soaking in Ag sol for 3 h. Ag nanoparticles are seen to be sparsely but almost evenly distributed over the Cu substrates. According to the separate UV/vis absorption spectra measured for Ag sol after adsorbing on 4-ABT/Cu, the surface coverage of Ag nanoparticles is estimated to be 1.8/μm^2; in this estimation, we considered the BET area of powdered copper to be 2.56 m^2/g. Figure 3b shows the FE-SEM image of 4-ABT/Cu after soaking in Au sol for 3 h. Au nanoparticles are also sparsely and evenly distributed over 4-ABT/Cu. The surface coverage of Au nanoparticles is also 1.8/μm^2. There is no question that the Ag and Au nanoparticles are bound directly to the amino groups of 4-ABT on copper. Their low surface coverage is associated with the electrostatic repulsive interaction of citrate-stabilized colloidal particles.[21,22]

Figure 3c shows the FE-SEM image of silica beads that have previously been treated with 4-APTMS and then soaked in Ag sol. The surface coverage of Ag nanoparticles on silica beads is comparable to that on copper powders. Most of the Ag nanoparticles are present on silica beads in isolated state as commonly as they are on copper powders. The FE-SEM image provides also evidence that a few Ag nanoparticles are present in an aggregated state. We have endeavored to obtain Raman spectra for (4-aminophenyl)silane monolayers assembled on silica beads, but we could obtain only featureless spectra. This

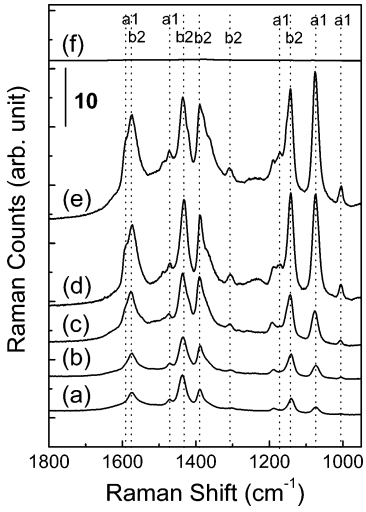

Figure 4. SERS spectra taken for Ag@4-ABT/Cu using (a) 488-, (b) 514.5-, (c) 568-, (d) 632.8-, and (e) 647-nm radiation as excitation source. (f) SERS spectrum of 4-ABT/Cu taken using 647-nm excitation, the same as in Figure 2b.

may indicate that the Ag nanoparticles adsorbed onto amino groups are neither hot particles nor hot clusters exhibiting huge SERS enhancement. Regarding these matters, it would be informative to compare the SERS spectral features of 4-APTMS and 4-ABT in Ag sol. In fact, 4-ABT can be readily adsorbed on Ag; thereby a very intense Raman spectrum is obtained in Ag sol (see Figures S1 and S2 of the Supporting Information). In contrast, 4-APTMS is a much weaker adsorbate so that it is not unreasonable to observe several tens times weaker SERS spectrum than that of 4-ABT. Although weak, the SERS peaks of 4-APTMS can be identified, however (see Figure S1). Considering the fact that the intrinsic Raman scattering cross-section of 4-APTMS is at best 1.5−2 times smaller than that of 4-ABT, the observation of SERS peaks of 4-APTMS in Ag sol is definitely associated with the formation of Ag clusters. If similar hot Ag clusters were formed on 4-APTMS assembled on silica beads, one would also observe SERS peaks, contrary to the actual experiment. On this ground, the Ag and Au nanoparticles adsorbed on 4-ABT/Cu are also presumed not to possess hot sites for induction of SERS.

Figure 4 shows a series of Raman spectra of 4-ABT/Cu taken using different excitation lasers after soaking in Ag sol for 3 h; hereafter, this system will be denoted Ag@4-ABT/Cu. The absolute intensities in Figure 4 are all referenced relative to those for silicon wafers used for instrument calibration. For reference, the Raman spectrum of 4-ABT/Cu obtained using 647-nm radiation prior to adsorbing Ag nanoparticles is also reproduced in Figure 4f with the same intensity scale. It is noticed that the Raman scattering intensity increases dramatically upon adsorbing Ag nanoparticles onto 4-ABT/Cu. The Raman scattering intensity is also noted to increase upon increase of the excitation wavelengths. Although the absolute peak intensity was not intense, similar excitation-wavelength dependence was observed even before adsorbing Ag nanoparticles onto 4-ABT/Cu, as mentioned previously. It has to be mentioned that sharply different excitation-wavelength dependence is observed when 4-ABT is adsorbed on Ag nanoparticles. As can be seen in the Ag sol SERS spectra (see Figure S2), the SERS peak of 4-ABT in Ag sol decreases as the excitation wavelength is increased gradually from 488 to 647 nm. If the dramatic intensity increase in Figure 4 was due to any Ag clusters formed on 4-ABT/Cu, the SERS peak should have diminished upon increase of the excitation wavelengths, as contrary to the actual observation.

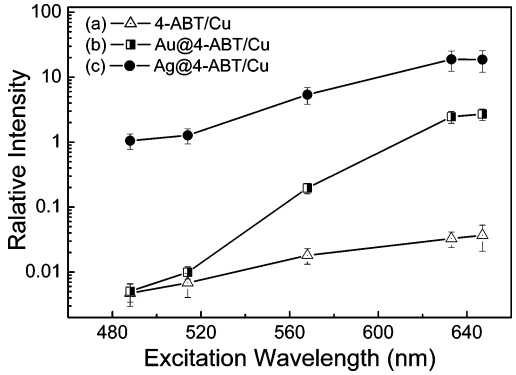

Figure 5. Excitation wavelength dependence of Raman scattering intensity of the 7a band for (a) 4-ABT/Cu, (b) Au@4-ABT/Cu, and (c) Ag@4-ABT/Cu. Raman scattering intensities are the average of 10 measurements.

Hence, the increase in the Raman scattering intensity observed herein must be attributed to the coupling of Ag nanoparticles with the copper substrate underneath. The observed Raman peaks are also summarized in Table 1.

As commonly as for 4-ABT/Cu, the b_2-type bands are observed distinctly in the Raman spectra of Ag@4-ABT/Cu. It is also seen that the a_1-type bands become intensified as a function of excitation wavelength. For instance, as shown in Figure 5c, the Raman scattering intensity of the 7a band at 1073 cm^{-1} increases by 220, 190, 300, 580, and 510 times upon adsorbing Ag nanoparticles onto 4-ABT/Cu when the excitation wavelength is increased gradually from 488 nm to 514.5, 568, 632.8, and 647 nm, respectively; see also Table 2. To evaluate the effect of Ag nanoparticles more quantitatively, we have to take account of the number of Ag nanoparticles actually sampled by the excitation lasers. Since the laser beam diameter is 1 μm, the actual area irradiated is 0.79 μm^2 so that the number of Ag nanoparticles sampled by the excitation laser will be 1.4, for the surface coverage of Ag nanoparticles is 1.8/μm^2. Considering then that the diameter of Ag nanoparticle is 50 nm, the area covered by 1.4 Ag nanoparticles will be 0.0028 μm^2. Denoting the Raman scattering intensity of 4-ABT/Cu sampled by a 1-μm-sized laser beam as I_o, the amount of signal contributed by 0.0028 μm^2 will be $0.0028I_o$. Representing, then, the Raman scattering intensity solely due to 1.4 Ag nanoparticles as I, the signal detected for the sample of Ag@4-ABT/Cu may be denoted $(1 - 0.0028)I_o + I = 0.9972I_o + I$, which is, for instance, 580 times greater than I_o when 632.8-nm radiation is used as the excitation source. In the latter case, it holds that $I = 580I_o$. The Raman scattering intensity enhancement caused by the adsorption of a single Ag nanoparticle would then be evaluated to be $(580I_o/0.0028I_o)(1/1.4) = 1.4 \times 10^5$. A similar calculation results in EF values per attachment of a single Ag nanoparticle of 5.5×10^4, 4.7×10^4, 7.5×10^4, and 1.3×10^5 following excitation at 488, 514.5, 568, and 647 nm, respectively; see also Table 2. These excessively large values suggest that the crevices or the gaps occurring with two or three nanoparticles in contact with one another are indeed "hot" sites for the induction of SERS via a huge EM enhancement mechanism.[5,6]

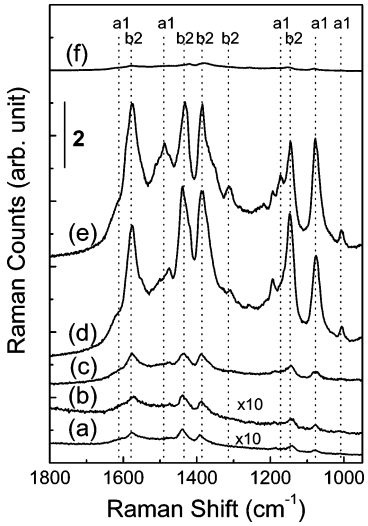

Figure 6. SERS spectra taken for Au@4-ABT/Cu using (a) 488-, (b) 514.5-, (c) 568-, (d) 632.8-, and (e) 647-nm radiation as excitation source. (f) SERS spectrum of 4-ABT/Cu taken using 647-nm excitation, the same as in Figure 2b.

The Raman scattering intensity increase is comparatively insignificant when Au nanoparticles are adsorbed, instead of Ag nanoparticles, onto 4-ABT/Cu. Figure 6 shows a series of Raman spectra of 4-ABT/Cu taken using different excitation lasers after soaking in Au sol for 3 h. For reference, the Raman spectrum of 4-ABT/Cu obtained using 647-nm radiation prior to adsorbing Au nanaoparticles is also reproduced in Figure 6f with the same intensity scale. In fact, as shown in Figure 5 (and Table 2), the Raman scattering intensity of the 7a band at 1078 cm^{-1} increases by 1.1, 1.5, 11, 34, and 73 times upon adsorbing Au nanoparticles onto 4-ABT/Cu when the excitation wavelength is increased from 488 nm to 514.5, 568, 632.8, and 647 nm, respectively. Recalling the fact that the surface coverage of Au nanoparticles on 4-ABT/Cu was the same as that of Ag nanoparticles with comparable sizes, the additional EF values due to the adsorption of a single Au nanoparticle should be 3.1×10^2, 4×10^2, 5.5×10^3, 1.8×10^4, and 1.8×10^4 in accordance with the excitation at 488, 514.5, 568, 632.8, and 647 nm, respectively. These values reveal once again that the crevices or the gaps occurring with two or three nanoparticles in contact with one another are hot sites for the induction of SERS via the EM enhancement mechanism.[5,6] However, the EF value for Au nanoparticles is about 2 orders of magnitude smaller than that for Ag nanoparticles when 488- or 514.5-nm radiation is used as the excitation source. As lasers with longer wavelengths are used, the EF value for Au nanoparticles becomes closer to that for Ag nanoparticles. For instance, the EF value for Au nanoparticles is about an order of magnitude

TABLE 2: Excitation Wavelength Dependence of Raman Scattering Intensity of the 7a Band of 4-Aminobenzenethiol on Cu before and after Attaching Ag and Au Nanoparticles (NPs)[a]

laser wavelength (nm)	intens for 4-ABT/Cu	intens after Ag bound	intens increase by Ag NPs	enhancement factor per Ag NP	intens after Au bound	intens increase by Au NPs	enhancement factor per Au NP
488	0.0047	1.1	220	5.5×10^4	0.0051	1.1	2.7×10^2
514.5	0.0068	1.4	190	4.7×10^4	0.0099	1.5	3.6×10^2
568	0.018	5.4	300	7.5×10^4	0.20	11	2.7×10^3
632.8	0.033	19	580	1.4×10^5	2.5	34	8.5×10^4
647	0.037	19	510	1.3×10^5	2.7	73	1.8×10^4

[a] Raman scattering intensities are the average of 10 measurements.

smaller than that for Ag nanoparticles at 568- and 632.8-nm excitation and then becomes about one-seventh for 647-nm excitation.

It is not clear at the moment why Au nanoparticles are ineffective to induce SERS for 488- and 514.5-nm excitation. Consulting the diffuse reflectance UV/vis spectrum of powdered copper, the absorption cutoff edge occurs at ~550 nm. Considering that the surface plasmon band for Au nanoparticles appears at >520 nm while that for Ag nanoparticles appears at ~420 nm, the electromagnetic coupling of the localized surface plasmon of Au nanoparticles with the surface plasmon polariton of Cu powders may be ineffective in the presence of electromagnetic radiation at ~500 nm.

4. Conclusion

We have examined the effect of Ag and Au nanoparticles on the Raman scattering intensity of 4-aminobenzenethiol (4-ABT) adsorbed on powdered copper substrates. The powdered copper itself is not an efficient SERS substrate, but Raman scattering intensity enhancement up to 2 orders of magnitude can readily be identified for 4-ABT adsorbed thereon. The latter enhancement is presumed to be due to the CT mechanism, taking account of the appearance of the b_2-type bands and their intensity variation as a function of excitation wavelength. Upon attaching Ag nanoparticles onto 4-ABT/Cu, dramatic high-intensity Raman scattering takes place. This is certainly due to the electromagnetic coupling between the localized surface plasmon of Ag nanoparticles and the surface plasmon polariton of the copper substrate underneath.[16,23,24] The additional EF value attainable by the attachment of a single Ag nanoparticle is as large as 1.4×10^5 at 632.8-nm excitation. This is in conformity with the current view that the crevices or the gaps between two or three nanoparticles in contact with one another must be "hot" sites for the induction of SERS via a huge EM enhancement mechanism.[5,6] When Au nanoparticles are attached onto 4-ABT/Cu, the Raman scattering intensity increase is smaller by 1/200−1/7 times than the case of attachment of Ag nanoparticles depending on the excitation wavelength. Although the reason for such a difference is not certain at the moment, the Ag-to-Cu coupling seems far more effective than the Au-to-Cu coupling for the induction of SERS. Finally, the fact that the size of the Ag nanoparticles (50 nm) was smaller than that of Ag-coated atomic force microscopy (AFM) tips usually employed in tip-induced SERS, but the SERS signal was observed only on Cu, not on dielectric silicon oxide, would indicate that tip-induced SERS should also work well on metallic substrates.

Acknowledgment. This work was supported by the Korea Research Foundation (KRF, Grant 2003-015-C00285).

Supporting Information Available: SERS spectra of 4-ABT and 4-APTMS in Ag sol. This material is available free of charge via the Internet at http://pubs.acs.org.

References and Notes

(1) Chang, R. K.; Furtak, T. E. *Surface Enhanced Raman Scattering*; Plenum Press: New York, 1982.
(2) Moskovits, M. *Rev. Mod. Phys.* **1985**, *57*, 783.
(3) Nie, S.; Emory, S. R. *Science* **1997**, *275*, 1102.
(4) Xu, H.; Bjerneld, E. J.; Käll, M.; Börjesson, L. *Phys. Rev. Lett.* **1999**, *83*, 4357.
(5) Futamata, M.; Maruyama, Y.; Ishikawa, M. *Vib. Spectrosc.* **2002**, *30*, 17.
(6) Jiang, J.; Bosnick, K.; Maillard, M.; Brus, L. *J. Phys. Chem. B* **2003**, *107*, 9964.
(7) Lecomte, S.; Matejka, P.; Baron, M. H. *Langmuir* **1998**, *14*, 4373.
(8) Campion, A.; Ivanecky, J. E., III; Child, C. M.; Foster, M. *J. Am. Chem. Soc.* **1995**, *117*, 11807.
(9) Doering, W. E.; Nie, S. *J. Phys. Chem. B* **2002**, *106*, 311.
(10) Ni, J.; Lipert, R. J.; Dawson, G. B.; Porter, M. D. *Anal. Chem.* **1999**, *71*, 4903.
(11) Kim, N. H.; Lee, S. J.; Kim, K. *Chem. Commun.* **2003**, 724.
(12) Cao, P.; Gu, R.; Tian, Z. Q. *Langmuir* **2002**, *18*, 7609.
(13) Chu, W.; LeBlanc, R. J.; Williams, C. T.; Kubota, J.; Zaera, F. *J. Phys. Chem. B* **2003**, *107*, 14365.
(14) Tian, Z. Q.; Ren, B.; Wu, D. Y. *J. Phys. Chem. B* **2002**, *106*, 9463.
(15) Zheng, J.; Zhou, Y.; Li, X.; Ji, Y.; Lu, T.; Gu, R. *Langmuir* **2003**, *19*, 632.
(16) Futamata, M.; Maruyama, Y.; Ishikawa, M. *J. Phys. Chem. B* **2004**, *108*, 13119.
(17) Lee, P. C.; Meisel, D. *J. Phys. Chem.* **1982**, *86*, 3319.
(18) Brunauer, S.; Emmett, P. H.; Teller, E. *J. Am. Chem. Soc.* **1938**, *60*, 309.
(19) Osawa, M.; Matsuda, N.; Yoshii, K.; Uchida, I. *J. Phys. Chem.* **1994**, *98*, 12702.
(20) Varsanyi, G. *Assignments for Vibrational Spectra of Seven Hundred Benzene Derivatives*; Wiley: New York, 1974.
(21) Grabar, K. C.; Freeman, R. G.; Hommer, M. B.; Natan, M. J. *Anal. Chem.* **1995**, *67*, 735.
(22) Grabar, K. C.; Smith, P. C.; Musick, M. D.; Davis, J. A.; Walter, D. G.; Jackson, M. A.; Guthrie, A. P.; Natan, M. J. *J. Am. Chem. Soc.* **1996**, *118*, 1148.
(23) Hutter, E.; Cha, S.; Liu, J.-F.; Park, J.; Yi, J.; Fendler, J. H.; Roy, D. *J. Phys. Chem. B* **2001**, *105*, 8.
(24) Kume, T.; Nakagawa, N.; Hayashi, S.; Yamamoto, K. *Solid State Commun.* **1995**, *93*, 171.